Magnetotelluric results along the N-S Curnamona seismic traverse to the east of Lake Frome, South Australia

P.R. Milligan
Onshore Energy & Minerals Division
Geoscience Australia
GPO Box 378 ACT Australia 2601
Peter.Milligan@ga.gov.au

F.E.M. Lilley
Research School of Earth Sciences
Australian National University
Canberra ACT Australia 0200
Ted.Lilley@anu.edu.au

SUMMARY

Magnetotelluric data were acquired for Geoscience Australia by contract along the north-south 08GA-C1 Curnamona seismic traverse to the east of Lake Frome from November 2008 to January 2009 as part of the Australian Government's Onshore Energy Security Program. 25 sites were spaced an average of 10 km apart, and five-component broadband data were recorded with a frequency bandwidth of 0.001 Hz to 250 Hz and dipole lengths of 100 m.

Apparent resistivity and phase plots are presented, along with dimensional analyses of the data based on rotational invariants, the representation of the data by the phase tensor, and Parkinson arrows. These analyses provide insight into the complexity of the Earth conductivity giving rise to the MT responses and are a useful precursor to modelling.

Key words: Magnetotelluric, apparent resistivity, conductivity, Parkinson arrow, phase ellipse, Curnamona

INTRODUCTION

Magnetotelluric (MT) data were acquired for Geoscience Australia by Quantec Geoscience on behalf of Terrex Seismic Pty Ltd along the north-south 08GA-C1-Curnamona seismic traverse to the east of Lake Frome from November 2008 to January 2009 at 25 sites with an average spacing of 10 km as part of the Australian Government's Onshore Energy Security Program (Figure 1). The southern end of the traverse crosses the Willyama Supergroup, while the northern end covers the Mt Painter region of the northern Flinders Ranges.

The MT method complements deep Earth seismic data by providing information of Earth electrical conductivity from near-surface to mantle depths (Simpson and Bahr, 2005). The seismic and MT geophysical methods, along with potential field methods of magnetics and gravity, are particularly required in regions such as the Curnamona Province, which is largely covered by surficial sediments and regolith, to help delineate the crustal architecture and enable evaluation of energy and mineral potential.

Previous Geomagnetic Depth Sounding (GDS) studies, with Telluric data at some sites, using magnetic variometer data have broadly mapped the axis of a crustal conductor, the Flinders Conductivity Anomaly (FCA), which crosses the present line at its southern extremity from the south-west and then trends to the north (Lilley and Tammemagi, 1972; Gough *et al*., 1974; Chamalaun, 1986). Seven resistivity soundings were also made in the area south of Lake Frome by Constable (1985) which showed that the surface sediments have very low resistivity.

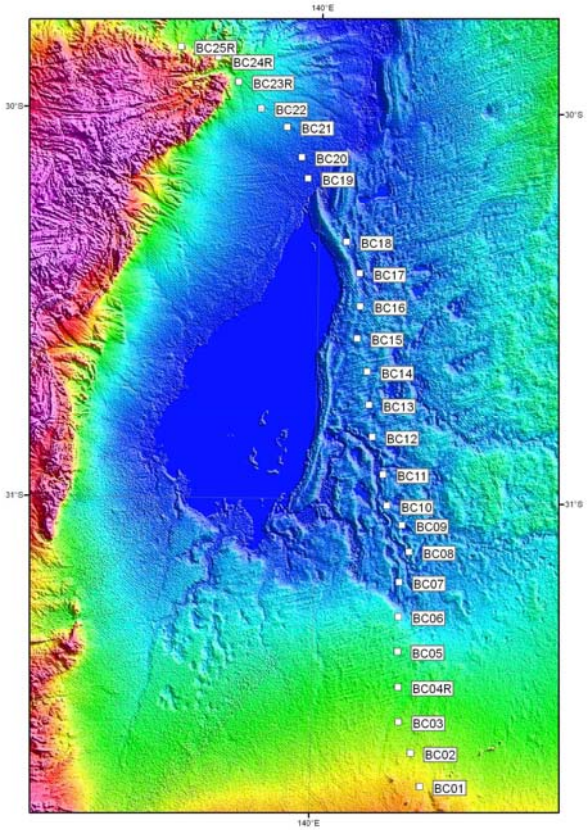

Figure 1. Locations of the 25 MT sites along the 08GA-C1 seismic line. The background image of elevation clearly shows Lake Frome to the south-east of the Flinders Ranges/Mt Painter region.

Except for the early work of Tammemagi and Lilley (1973), the only previous publicly available MT data for this region near the seismic line are by Adam (2007), who recorded long-period MT and GDS data across three profiles in the Olary and Broken Hill domains, to the east of the current traverse. The GDS data showed a response to the FCA, and resistivity profiles from inversion of the MT data showed an increase in crustal resistivity from the Olary to Broken Hill domains across the Mundi Mundi Fault.

METHOD AND RESULTS

The MT method uses natural time variations of the geomagnetic and geoelectric fields to infer Earth conductivity with depth. Time variations of Earth's magnetic field over a range of frequencies are the source field, which induces electric currents in Earth over a range of depths depending upon the frequencies measured and the conductivity. Source-field variations are measured by two orthogonal induction coils, while the electric field response is measured as electric potential at orthogonal pairs of electrodes. A further response, the vertical magnetic field, is also measured by using a vertically oriented induction coil; this procedure enables GDS parameters to be calculated.

Broadband data were acquired between 25 November 2008 and 27 January 2009 for Geoscience Australia by contract at 25 sites spaced on average 10 km apart. Five components (three magnetic and two electric) were recorded with a frequency bandwidth of 0.001 Hz to 250 Hz and dipole lengths of 100 m. Final data were supplied as auto- and cross-power spectral estimates in industry standard EDI files (Stockill *et al*., 2009). From these data, the complex frequency-dependent elements of the MT impedance tensor and subsequently apparent resistivity and phase curves for the two modes XY and YX are generated, along with the tipper function (Txr Txi & Tyr Tyi) sounding curves. Figure 2 shows an example of these curves for site BC02.

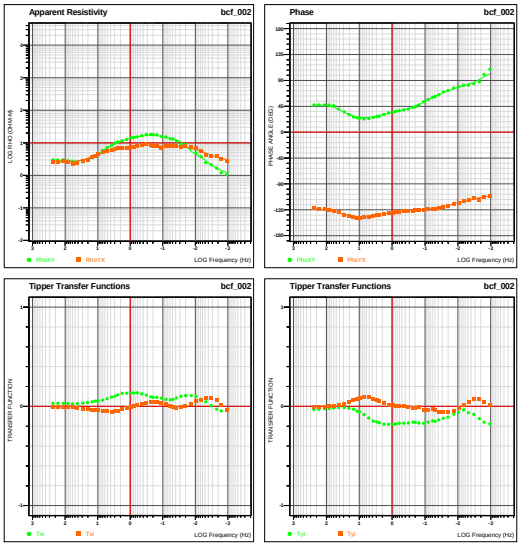

Figure 2. Example from site BC02 of apparent resistivity, phase (XY and YX) and tipper transfer function (Txr, Txi, Tyr, Tyi) sounding curves (from Stockill *et al*., 2009).

Processed data of apparent resistivity and phase values are conveniently displayed as pseudosections, in which the horizontal axis represents distance along the profile and the vertical axis represents frequency, with higher frequencies to the top (shallower responses). Figure 3 shows pseudosections of the two modes, XY and YX, for both apparent resistivity and phase.

Major features of the electrical conductivity structure beneath the profile are visible in these sections. Conducting sediments of the Frome Embayment are clearly visible at the top of the sections, with a suggestion of thickening to the north. Beneath these sediments there is a resistive layer in most of the central part of the section, while to the south there is a deeper conductive zone and to the north a deeper resistive zone.

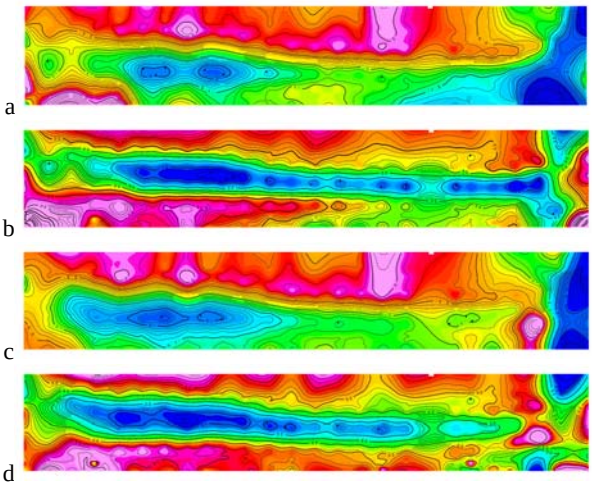

Figure 3. Pseudosections of apparent resistivity and phase. (a) top, xy apparent resistivity, (b) xy phase, (c) yx apparent resistivity, (d) yx phase. For (a) and (c) colours represent $\log_{10}$ of conductivity; For (b) and (d) phase data are in degrees 0 to 90. Blue low to red high. The width of the section is 240 km, with south, left to north, right; the Y-axis represents frequency, with low, bottom to high, top.

A method of displaying the data as a depth section is provided by calculation of the Bostik transform (Bostick, 1977; Goldberg and Rotstein, 1982). This transform provides an initial approximate 1D interpretation of the data, as a prelude to more sophisticated modelling, to highlight gross details in the conductivity distribution. Figure 4 shows sections derived from Bostick-transformed data.

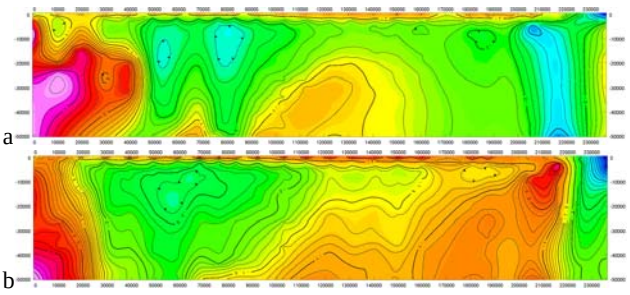

Figure 4. Pseudosections of the Bostick transform. (a) top, xy mode and (b) bottom, yx mode. The data represent the $\log_{10}$ of the conductivity with blue low to red high. The width of the section is 240 km with south, left to north, right; the depth of the section is 50 km.

The two sections shown in Figure 4 for the xy and yx modes display data varying smoothly in space with several common features between the two modes. Such consistency provides confidence that the features represent actual variations in the subsurface conductivity.

The main features in common between the modes are:
(1) The high near-surface conductivity values in the central part of the section which correlate with conductive surface sediments. The depth of this conductive zone increases towards the north until a more resistive surface is encountered. At the southern end, the depth decreases, but the conductivity remains higher than at the northern end.
(2) The more resistive zone beneath the surface sediments, from approximately 20 km in the south to 110 km in the north.

This zone is prominent, extending in depth to 40 km in some parts. North of 110 km it continues as a horizontal layer up to about 200 km, more prominently in the yx mode than in the xy mode.
(3) A deep zone of higher conductivity in the south. While present in both modes, the details are different, probably representing the complex nature of Earth conductivity here.
(4) A zone of higher conductivity in the centre of the section beneath the more resistive zone of (2), extending deeper from about 20 km.

A major difference between the two modes is in the north of the section, where the sites are located across the boundary of the northern Flinders Ranges. Both modes show an almost vertical variation in conductive property here, but the xy mode displays a vertical resistive zone, whereas the yx mode shows a gradient from higher conductivity to lower conductivity. Dimensional analysis of the data from these sites, as described below, has shown that the deeper conductivity is three-dimensional in nature, and this result explains the disparity in the Bostick transform results.

Estimates of the dimensionality of Earth conductivity structure as represented by the MT impedance tensor may be made by a study of the rotational invariants of the impedance tensor (Lilley, 1998; Weaver *et al*., 2000; Lilley and Weaver, 2008; Lilley and Weaver, 2010). A convenient program (WALDIM) to compute the invariants and estimate strike directions and various types of dimensionality has been published by Marti *et al*. (2009). Eight dimensionality types are computed; 0 (undetermined), 1 (1D), 2 (2D), 3 (3D/2D only twist), 4 (3D/2D general), 5 (3D), 6 (3D/2D with diagonal regional tensor) and 7 (3D/2D or 3D/1D indistinguishable).

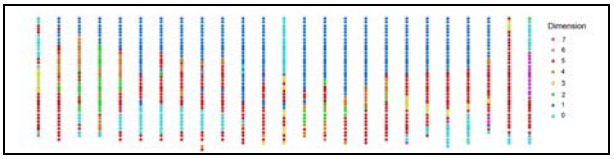

Figure 5. Coloured circles representing dimensionality as determined from the WALDIM program. Horizontal axis represents site locations with south, left to north, right; the Y-axis represents frequency, with low, bottom to high, top.

The dimensionality as represented by the numbers 0 to 7 can be displayed as coloured symbols with the horizontal axis representing site locations along the profile, and the vertical axis the log of the frequency, so that the highest frequency is at the top. Figure 5 shows such a plot, in which colours blue and green represent 2D and less, with 1D represented by darker blue. Yellow to red and purple represent higher and/or more complex dimensions in which 1D and 2D modelling will be problematic. Higher frequencies in the central part of the section have responses from a 1D Earth, mainly resulting from the near-surface sediments of the Frome Embayment.

Information regarding lateral variations in subsurface conductivity can be gained from study of Parkinson Arrows (Parkinson, 1959). These arrows relate changes in the vertical magnetic field to changes in the horizontal fields as a complex function of frequency, and point by convention to regions of higher conductivity. The length of the arrow is a function both of the strength of the currents that give rise to the vertical field variations, and the distance of the measuring site from the induced currents. Responses from shallow sources that are essentially 1D have very small arrows and both geological strike and arrow directions become meaningless.

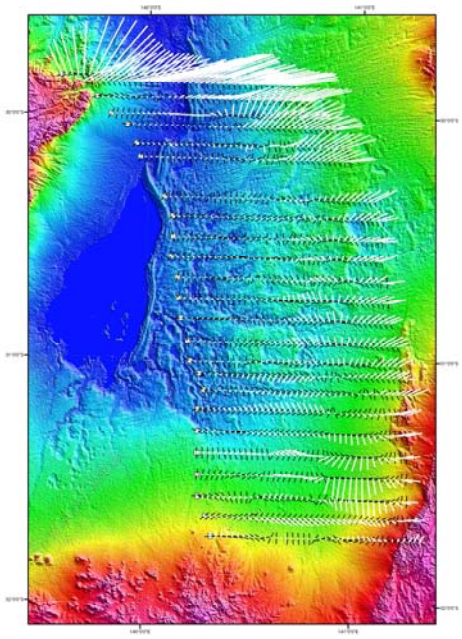

Figure 6. In-phase Parkinson Arrows (white) and strike directions (black), with highest frequency at left on site symbol (white square), lowest frequency to right.

Strike directions and arrows displayed in Figure 6 show a variation in direction and length, both with frequency and spatially. There is a relatively strong response in the north for sites in the Flinders Ranges which may result from currents concentrated around this sharp geological boundary. At low frequencies all the arrows tend to point in a north-east to east direction; this behaviour may be due to the previously-mapped FCA.

The phase-tensor approach to MT analysis of Caldwell *et al*. (2004) is useful in helping determine both strike and dimensionality of MT data independently of distortion effects such as static shift. No assumption is made about the underlying conductivity distribution in calculation of the phase tensor, which is depicted graphically as an ellipse.

Phase tensor ellipses have been calculated for data from the 25 MT sites for each period (Figure 7). The ellipses are coloured by skew angle value, and if this is greater than a few degrees then the data for that period must be considered resulting from a 3D conductivity distribution. Most of the ellipses in the central part of the traverse are circular for short periods, with the radii decreasing from the shortest periods to mid-range periods, where they become minimal before increasing again and the ellipses then become more elongate. The skew angle of these circles is also small. Thus, they represent essentially 1D data, with conductivity decreasing with depth from the surface. There is an elongate zone with minimal circle diameters in the mid-period range which represents a subsurface region of relatively low conductivity.

A second obvious feature is the change in character of the ellipses for sites at both extremities of the traverse. The ellipses increase in size with depth, are more elliptical, and the

skew angles are greater than the mid-traverse values for all periods. Thus, the conductivity represented by these ellipses is more complex and 3D. For the longest periods at all sites the phase tensors are represented by quite elliptical figures with high skew angles.

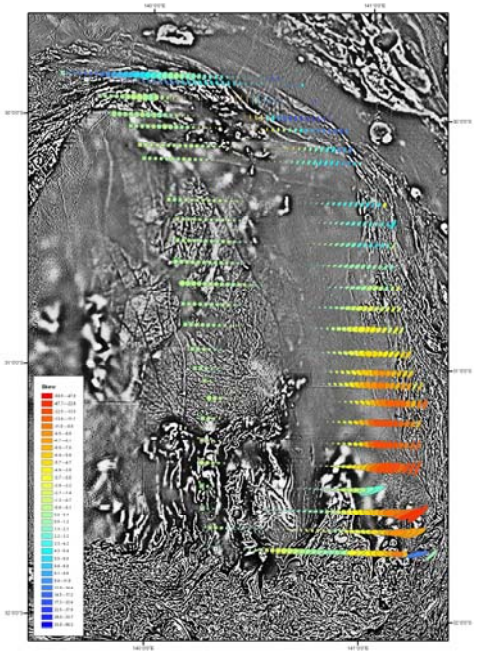

Figure 7. Phase tensor ellipses, coloured by skew angle, for each site and period, with the shortest period centred on the site symbol. Background image is of the second vertical derivative of the total magnetic intensity, highlighting near-surface short-wavelengths of aeromagnetic data.

CONCLUSIONS

Broadband MT data acquired along the 08GA-C1 seismic line have been presented and analysed in terms of pseudosections, dimension, Parkinson arrows and phase ellipses. These analyses indicate that near-surface conductive sediments are well-resolved, with some thickening to the north. A resistive layer underlies the sediments in the central part of the section. Across the Flinders Ranges in the north the data are more complex, and indicate higher resistivity from shallow to deeper levels. In the south, across the Willyama Supergroup, there is a more conductive zone, probably complicated by the FCA. Each method of analysis confirms the major features of the subsurface conductivity, and provides useful information for the next stage of inverse modelling.

ACKNOWLEDGMENTS

We thank the Seismic Acquisition and Processing Project of the Onshore Energy and Minerals Division, Geoscience Australia, and in particular Jenny Maher, for supporting this project. PRM publishes with permission of the Chief Executive Officer, Geoscience Australia.

REFERENCES

Adam, H., 2007, A magnetotelluric survey of the Broken Hill and Olary domains: Honours thesis, School of Earth and Environmental Sciences, University of Adelaide.

Bostick, F.X., 1977, A simple and almost exact method of MT analysis (abstract): Workshop on Electrical Methods in Geothermal Exploration, Snowbird, Utah, 1976.

Caldwell, T.G., Bibby, H.M. and Brown, C., 2004, The magnetotelluric phase tensor: Geophysical Journal International, 158, 457-469.

Chamalaun, F.H., 1986, Extension of the Flinders Ranges anomaly: Exploration Geophysics, 17, 31.

Constable, S.C., 1985, Resistivity studies over the Flinders conductivity anomaly, South Australia: Geophys. J. R. astron. Soc., 83, 775-786.

Goldberg, S and Rotstein, Y., 1982, A simple form of presentation of magnetotelluric data using the Bostick Transform: Geophysical Prospecting, 30, 211-216.

Gough, D.I., McElhinny, M.W. and Lilley, F.E.M., 1974, A magnetometer array study in southern Australia: Geophys. J. R. astron. Soc., 36, 345-362.

Lilley, F.E.M., 1998, Magnetotelluric tensor decomposition: Part 1, theory for a basic procedure: Geophysics, 63, 1885-1897.

Lilley, F.E.M. and Tammemagi, H.Y., 1972, Magnetotelluric and geomagnetic depth sounding methods compared (in southern Australia): Nature Physical Science, 240, 184-187.

Lilley, F.E.M. and Weaver, J.T., 2008, Invariants of rotation of axes and indicators of dimensionality in magnetotellurics: In: Ritter, O. and Brasse, H. (Eds) "Proceedings of the 22nd Colloquium of Electromagnetic Depth Research, Decin, Czech Republic", ISSN 0946-7467, 18-26.

Lilley, F.E.M. and Weaver, J.T., 2010, Phases greater than 90 deg in MT data: Analysis using dimensionality tools: Journal of Applied Geophysics, 70, 9-16.

Martí, A., Queralt, P., Jones, A.G. and Ledo, J., 2005, Improving Bahr's invariant parameters using the WAL approach: Geophysical Journal International., 163, 38-41.

Parkinson, W.D., 1959, Directions of rapid geomagnetic fluctuations: Geophys. J. R. astron. Soc., 2, 1-14.

Simpson, F and Bahr, K., 2005, Practical Magnetotellurics: Cambridge University Press.

Stockill, J., Brown, D., Scappin, S., Retallick, T. & Gharibi, M., 2009, Geophysical Survey Logistics report (v.2), regarding the Quantec Spartan Tensor Magnetotelluric Survey over the Curnamona MT Project, near Arkaroola, South Australia, Australia, on behalf of Terrex Seismic Pty Ltd, Perth, WA, Australia.

Tammemagi, H.Y and Lilley, F.E.M., 1973, A magnetotelluric traverse in southern Australia: Geophys. J. R. astron. Soc., 31, 433-445.

Weaver, J.T., Agarwal, A.K. and Lilley, F.E.M., 2000, Characterisation of the magnetotelluric tensor in terms of its invariants: Geophysical Journal International, 141, 321-33.